控制与决策
Control and Decision

带输出死区的多智能体系统预设时间事件触发式协同控制

王建晖, 邹涛, 张春良, 穆朝絮, 刘治

引用本文:
王建晖,邹涛,张春良,穆朝絮,刘治. 带输出死区的多智能体系统预设时间事件触发式协同控制[J]. 控制与决策, 2023, 38(2): 441-449.

在线阅读 View online: https://doi.org/10.13195/j.kzyjc.2021.0399

带输出死区的多智能体系统预设时间事件触发式协同控制

王建晖[1], 邹 涛[1†], 张春良[1], 穆朝絮[2], 刘 治[3]

(1. 广州大学 机械与电气工程学院，广州 510006；2. 天津大学 电气自动化与信息工程学院，天津 300072；3. 广东工业大学 自动化学院，广州 510006)

摘 要: 针对带有输出死区的多智能体系统的一致性控制问题,提出一种可预设时间的事件触发式协同控制方法. 输出死区现象普遍存在于实际系统,对控制回路中负反馈调节影响较大,会导致系统控制性能的下降. 为此,通过结合 Nussbaum 函数对输出死区特性进行补偿,以削弱其对系统性能的影响,但上述问题解决的同时也会加剧对系统控制传输资源的占用. 由于多智能体系统依靠智能体之间频繁的信息交互实现控制目标,自身传输资源有限. 考虑到实际系统的限制,利用事件触发控制策略节省系统的控制传输资源. 更进一步,为有效提高系统性能,使系统能够快速达到稳定,引入一类转换函数进行系统变换,实现系统同步误差在预设时间内收敛于紧集的目标. 理论分析和仿真结果验证了所提出方法的有效性.

关键词: 多智能体系统；输出死区；Nussbaum 函数；预设时间；事件触发；协同控制

中图分类号: TP273 **文献标志码:** A

DOI: 10.13195/j.kzyjc.2021.0399

引用格式: 王建晖,邹涛,张春良,等. 带输出死区的多智能体系统预设时间事件触发式协同控制 [J]. 控制与决策, 2023, 38(2): 441-449.

Prescribed setting time event-triggered synergetic control of multiagent systems with output dead-zone

WANG Jian-hui[1], *ZOU Tao*[1†], *ZHANG Chun-liang*[1], *MU Zhao-xu*[2], *LIU Zhi*[3]

(1. College of Mechanical and Electrical Engineering，Guangzhou University，Guangzhou 510006，China；2. College of Electrical Automation and Information Engineering，Tianjin University，Tianjin 300072，China；3. College of Automation，Guangdong University of Technology，Guangzhou 510006，China)

Abstract: Aiming at the problem of consensus control of multi-agent systems with dead-zone outputs, this paper proposes a prescribed settling time event-triggered consensus control method. The dead-zone output phenomenon is common in actual systems. Its negative feedback adjustment has a great influence on the control loop, which will lead to the decline of the system control performance. For this reason, the dead-zone output characteristic is compensated by combining the Nussbaum function to weaken its impact on system performance. However, solving the above problems will also increase the occupation of system control transmission resources. Since the multi-agent system relies on frequent information interaction between agents to achieve control goals, its own transmission resources are limited. Taking into account the limitations of the actual system, the event-triggered control strategy is applied to economize system control transmission resources. Furthermore, to effectively improve the performance of the system and enable the system to quickly reach stability, a type of conversion function is introduced to perform system transformation, which achieves the goal of system synchronization error converging to a compact set within prescribed settling time. Theoretical analysis and simulation results verify the effectiveness of the proposed method.

Keywords: multi-agent systems; dead-zone output; Nussbaum function; prescribed setting time; event-triggered control; consensus control

---

收稿日期: 2021-03-09；**录用日期:** 2021-11-11.

基金项目: 国家自然科学基金项目 (51775122, 51505092)；广东省教育厅创新人才项目 (2018KQNCX197)；广东省教育厅创新强校项目 (2020KTSCX097)；广东省自然科学基金项目 (2019A1515110995)；广州市科技计划项目 (202002030286)；广州大学校内项目 (YG2020009).

责任编委: 王燕舞.

[†]通讯作者. E-mail: tzou@gzhu.edu.cn.

0 引 言

由于物理器件非线性特性、运行条件和检测精度等因素的限制,输出死区现象普遍存在于实际系统. 输出死区现象对系统负反馈通道影响较大,会很大程度上削弱系统的控制性能[1-5]. 针对非严格反馈下不确定切换系统涉及的输出死区问题,文献[1-2]利用Nussbaum函数对输出死区特性进行处理,构造相应的控制策略,从而保证系统控制性能. 文献[3]利用Lyapunov-Krasovskii函数的中值定理对系统输出死区特征进行补偿. 上述方法可以较好地处理系统输出死区现象,因此,采用适当的方法补偿系统输出死区特性对提升系统控制性能具有重大影响.

对输出死区现象的补偿,不可避免地会加剧对系统控制传输资源的占用. 多智能体系统往往应用于无人机编队、多机械臂协同装备、交通车辆控制等领域,受限于成本等因素,每个多智能体的实际通讯能力是有限的. 为避免因通讯带宽被过多占用导致通讯时延、丢包甚至中断,学者们展开了大量探索[6-14]. 针对分布式多智能体系统,文献[7]提出了一种分布式事件触发采样传输策略,可有效降低多智能体之间的通讯成本,减小计算压力. 文献[11]利用事件触发传输方法降低所考虑系统数据传输的频率. 基于事件触发策略,文献[13]研究了切换拓扑异构多智能体的协同输出调节问题. 由上述现有成果可知,事件触发机制可以很好地降低通讯频率,节约控制传输资源,对于信息交互频繁的复杂系统尤为适用.

此外,现有的大部分控制方法只能得到当时间趋于无穷时系统状态收敛于平衡点的结论,即系统渐近稳定[15]. 但是,对于很多实际问题而言,在预设时间内快速达到要求的稳定状态,才是最符合人们期望的. 鉴于此,有限时间稳定性吸引了学者们的广泛关注[15-20]. 文献[15]对有限时间理论的发展进行了回顾与展望. 文献[18]对齐次系统的有限时间稳定性进行了分析. 针对非三角随机非线性系统,文献[19]进行了模糊自适应有限时间控制方法设计. 上述方法从理论上证明了系统可以在有限时间内到达平衡点,但无法给出“有限时间”的确切值. 由于多智能体系统往往复杂度较高,为实现一致性控制等目标,对系统稳定时间要求较高[21-26]. 文献[21]针对多智能体的一致性问题,结合有限时间控制理论,设计了有限时间扰动观测器. 文献[23]研究了一类带外界扰动的二阶非线性多智能体系统的有限时间控制问题. 因此,探究如何在预设时间内收敛具有重要的理论意义及工程应用前景.

受上述研究工作的启发,本文研究带有输出死区的多智能体系统一致性跟踪问题. 与现有控制方法相比,所提出方法同时考虑系统的输出死区特性和有限的通讯资源,利用Nussbaum函数和事件触发机制进行综合设计. 此外,通过引入一类转换函数进行系统变换,保证系统同步误差在预设时间内收敛于紧集,有效提高系统的控制性能.

1 预备知识与问题描述

1.1 图 论

包含N个多智能体的多智能体系统之间的信息交互将通过有向图$\mathcal{G}=(\mathcal{V},\varepsilon)$描述. 其中:$\mathcal{V}=\{\mathcal{V}_1,\mathcal{V}_2,\ldots,\mathcal{V}_N\}$为非空节点数,$\varepsilon\subseteq\mathcal{V}\times\mathcal{V}$为节点的边. $\mathcal{A}=[a_{ij}]_{N\times N}$为有向图$\mathcal{G}$的邻接矩阵. $(\mathcal{V}_j,\mathcal{V}_i)\in\varepsilon$表示节点$j$到节点$i$的边. 当节点$j$的信息可以被传递到节点$i$时,$a_{ij}>0$,否则$a_{ij}=0$. 此外,$\mathcal{L}=\mathcal{D}-\mathcal{A}\in R^{N\times N}$为拉普拉斯矩阵,对角矩阵$\mathcal{D}=\mathrm{diag}(d_1,d_2,\ldots,d_N)\in R^{N\times N}$,节点$i$的度为$d_i=\sum\limits_{j=1}^{N}a_{ij}$.

引理1[1] 定义$\mathcal{B}=\mathrm{diag}\{b_i\}\in R^{N\times N}$,$b_i\geqslant 0$,则矩阵$\mathcal{L}+\mathcal{B}$非奇异.

1.2 系统描述

本文考虑具有N个跟随者的多智能体系统,其模型可以描述为

$$\begin{cases}\dot{x}_{i,k}=x_{i,k+1}+f_{i,k}(x_i),\\ \dot{x}_{i,n}=u_i+f_{i,n}(x_i),\\ y_i=\mathrm{DZ}(x_{i,1}).\end{cases}\tag{1}$$

其中:$x_i=[x_{i,1},x_{i,2},\ldots,x_{i,n}]^{\mathrm{T}}\in R^n$为状态变量,$f_{i,k}(x_i)$为未知光滑函数,$u_i$为系统控制输入,$y_i=\mathrm{DZ}(x_{i,1})$为系统死区输出,$i=1,2,\ldots,N$.

假设1[27] 本文所考虑的多智能体系统中虚拟领导者的输出y_d及其n阶导数都是连续且有界的.

系统的死区特性可以描述为

$$\mathrm{DZ}(x_{i,1})=\begin{cases}w_r(x_{i,1}-d_r),\ x_{i,1}>d_r;\\ 0,\ d_l<x_{i,1}<d_r;\\ w_l(x_{i,1}-d_l),\ x_{i,1}<d_l.\end{cases}\tag{2}$$

其中:$w_r>0,w_l>0,d_r>0,d_l<0$等为死区参数.

由式(1)和(2)可得

$$x_{i,1}=\mathrm{DZ}^{-1}(y_i)=\\ \frac{y_i+w_rd_r}{w_r}\psi_r(y_i)+\frac{y_i+w_ld_l}{w_l}\psi_l(y_i),\tag{3}$$

$$\psi_r(y_i)=\frac{1}{2\pi}(\pi+2\arctan(k_0y_i)),\tag{4}$$

$$\psi_l(y_i)=\frac{1}{2\pi}(\pi-2\arctan(k_0y_i)),\tag{5}$$

其中$k_0 > 0$为设计参数. 通过调整k_0,可提升对系统输出死区特性的逼近精度.

由式(3)～(5)可得

$$\frac{\mathrm{d}x_{i,1}}{\mathrm{d}y_i}=\frac{1}{w_r}\frac{\pi+2\arctan(k_0y_i)}{2\pi}+\frac{1}{w_r}\frac{k_0y_i}{\pi(1+k_0^2y_i^2)}+ d_r\frac{k_0}{\pi(1+k_0^2y_i^2)}+\frac{1}{w_l}\frac{\pi-2\arctan(k_0y_i)}{2\pi}- \frac{1}{w_l}\frac{k_0y_i}{\pi(1+k_0^2y_i^2)}-d_l\frac{k_0}{\pi(1+k_0^2y_i^2)}. \tag{6}$$

定义$w_{\max}=\max\{w_l,w_r\}$, $w_{\min}=\min\{w_l,w_r\}$, $\bigwedge_l=\pi-2\arctan(x_i)$, $\bigwedge_r=\pi+2\arctan(x_i)$,则有

$$G(x)=\frac{\mathrm{d}x_{i,1}}{\mathrm{d}y_i}= \frac{w_l\bigwedge_l(1+x_i^2)+w_r\bigwedge_l(1+x_i^2)}{2\pi w_rw_l(1+x_i^2)}+ \frac{2(w_l-w_r)x_i}{2\pi w_rw_l(1+x_i^2)}+\frac{2w_lw_r\Delta dk_{x_i}}{2\pi w_rw_l(1+x_i^2)}, \tag{7}$$

其中$\Delta d=d_r-d_l$.

情况1　当$x_i\leqslant 0$,定义

$$g(x)= \frac{1}{w_{\max}}+\frac{2(w_{\max}-w_{\min})x_i+2w_lw_r\Delta dk_{x_i}}{2\pi w_rw_l(1+x_i^2)}. \tag{8}$$

由式(7)和(8)可知, $g(x_i)\leqslant G(x_i)$. 当

$$x_i=-\frac{w_{\max}w_{\min}\Delta dk}{w_{\max}-w_{\min}}$$

时, $g(x_i)$存在最小值. 因此有

$$\frac{1}{w_{\max}}\leqslant g(x_i)\leqslant G(x_i). \tag{9}$$

情况2　当$x_i>0$时,与情况1相似,可得式(9).

综上分析,可得到如下结论:

$$0<\frac{1}{w_{\max}}<\frac{\mathrm{d}x_{i,1}}{\mathrm{d}y_i}\Rightarrow 0<\frac{\mathrm{d}y_i}{\mathrm{d}x_{i,1}}<w_{\max}. \tag{10}$$

设$K(t)=\dfrac{\mathrm{d}y_i}{\mathrm{d}x_{i,1}}$,则有

$$\dot{y}_i=\frac{\mathrm{d}y_i}{\mathrm{d}x_{i,1}}\dot{x}_{i,1}=K(t)\dot{x}_{i,1}, \tag{11}$$

其中$0<K(t)<w_{\max}=\max\{w_l,w_r\}$.

1.3　模糊逻辑系统

对于所考虑系统中存在的未知函数,利用模糊逻辑系统对其进行逼近处理. 模糊逻辑系统主要由如下形式的if-then规则构成:

$$R^l:\ \text{if } x_1 \text{ is } F_1^l \text{ and } \dots \text{ and } x_n \text{ is } F_n^l;$$
$$\text{then } Y \text{ is } G^l,\ l=1,2,\dots,N^n.$$

其中:模糊逻辑系统的输入输出分别为$X\in[x_1,x_2,\dots,x_n]^{\mathrm{T}}\in R^n$和$Y\in R$, F_i^l和G^l为模糊集, N为模糊规则的数目.

进一步,模糊逻辑系统的输出可以表示为

$$Y(X)=\frac{\sum_{l=1}^{N}\varPhi_l\prod_{i=1}^{n}\mu_{F_i^l}(x_i)}{\sum_{l=1}^{N}\left[\prod_{i=1}^{n}\mu_{F_i^l}(x_i)\right]}. \tag{12}$$

其中: $\varPhi_l=\max\limits_{y\in R}\mu_{G^l}(y)$, $\varPhi=[\varPhi_1,\varPhi_2,\dots,\varPhi_N]^{\mathrm{T}}$.

定义$\zeta_l(X)=\dfrac{\sum_{l=1}^{N}\mu_{F_i^l}(x_i)}{\sum_{l=1}^{N}\left[\prod_{i=1}^{n}\mu_{F_i^l}(x_i)\right]}$, $\xi=[\xi_1,\xi_2,\dots,\xi_N]^{\mathrm{T}}$,则模糊逻辑系统可以表示为如下形式:

$$y(X)=\varPhi^{\mathrm{T}}\zeta(X). \tag{13}$$

引理2[27]　若$f(X)$为连续函数,则对于$\forall\chi>0$,存在如下不等式:

$$\sup_{X\in\varOmega}|f(X)-\varPhi^{\mathrm{T}}\zeta(X)|\leqslant\chi, \tag{14}$$

其中χ为逼近误差的界.

1.4　转换函数概述

为了达到系统在预设时间内到达稳态的控制目标,引入如下一类非线性转换函数:

$$\lambda_i(t)=\begin{cases}\dfrac{T^2\mathrm{e}^{\nu t}}{\left(1-\dfrac{\varTheta}{\varPsi}\right)(T-t)^2+\dfrac{\varTheta}{\varPsi}T^2\mathrm{e}^{\nu t}},\ 0\leqslant t<T;\\[2ex] \dfrac{\varTheta}{\varPsi},\ t\geqslant T.\end{cases} \tag{15}$$

其中: $T>0$为预设时间; $\varTheta$、$\varPsi$和$v>0$均为设计参数, $\varTheta\gg\varPsi$.

1.5　Nussbaum函数性质

若函数$N(\xi)$满足如下性质,则称其为Nussbaum函数:

$$\lim_{s\to+\infty}\sup\frac{1}{s}\int_0^s N(\xi)\mathrm{d}\xi=+\infty, \tag{16}$$

$$\lim_{s\to-\infty}\inf\frac{1}{s}\int_0^s N(\xi)\mathrm{d}\xi=-\infty. \tag{17}$$

从上述定义易知, $\exp(\xi^2)$、$\xi^2\cos(\xi)$等均为Nussbaum函数.

引理3[28]　令$V(\cdot)$、$\xi(\cdot)$为定义在$[0,t_f)$上的光滑函数, $V(t)\geqslant 0$, $N(\cdot)$为光滑的Nussbaum函数. 若如下不等式成立:

$$V(t)\leqslant c_0+\int_0^t(g(x(\tau))N(\xi)+1)\dot{\xi}\mathrm{e}^{-c_1(t-\tau)}\mathrm{d}\tau. \tag{18}$$

其中: c_0、c_1为设计参数, $0<|g(x(\tau))|<l<\infty$, l为常数. 则$\int_0^t(g(x(\tau))N(\xi)+1)\dot{\xi}\mathrm{e}^{-c_1(t-\tau)}\mathrm{d}\tau$、$V(t)$、$\xi(t)$在区间$[0,t_f)$有界.

定义1　多智能体系统的同步误差可以描述为

$$e_i = b_i(y_i - y_d) + \sum_{j=1}^{N} a_{ij}(y_i - y_j), \qquad (19)$$

其中$b_i \geqslant 0$为节点i到领导者的边的权重. 当节点i接收到领导者信息时, $b_i > 0$, 否则$b_i = 0$. 值得注意的是, 系统中最少有一个节点将会接收到领导者的同步信息.

引理 4[29]　对于$\forall(x, y) \in R^2$, 如下不等式成立:

$$xy \leqslant \frac{\xi}{a}|x|^a + \frac{1}{b\xi^b}|y|^b. \qquad (20)$$

其中: $a > 1, b > 1, \xi > 0, (a-1)(b-1) = 1$.

2　预设时间事件触发式协同控制设计

定义如下变换系统:

$$\begin{cases} z_{i,1} = \lambda_i e_i, \\ z_{i,k} = x_{i,k} - \alpha_{i,k-1}, \end{cases} \qquad (21)$$

其中$\alpha_{i,k-1}$为虚拟控制器, 其设计将在后续给出, $i = 1, 2, \ldots, N, k = 2, 3, \ldots, n$. 对式(19)求导, 可得

$$\dot{e}_i = (b_i + d_i)K(t)[f_{i,1}(x_i) + x_{i,2}] - b_i\dot{y}_d - \sum_{j=1}^{N} a_{ij}K(t)(f_{j,1}(x_i) + x_{j,2}). \qquad (22)$$

step 1: 构造如下 Lyapunov 函数:

$$V_{i,1} = \frac{1}{2}z_{i,1}^2 + \frac{1}{2\ell_{i,1}}\tilde{P}_{i,1}^{\mathrm{T}}\tilde{P}_{i,1}. \qquad (23)$$

其中: $\ell_{i,1} > 0$为设计参数; $\tilde{P}_{i,1} = P_{i,1} - \hat{P}_{i,1}$, $P_{i,1}$为自适应变量, $\hat{P}_{i,1}$为$P_{i,1}$的估计值.

由式(23)可得

$$\dot{V}_{i,1} = z_{i,1}\Big(\dot{\lambda}_i e_i + \lambda_i\Big((b_i + d_i)K(t)(f_{i,1}(x_i) + x_{i,2}) - b_i\dot{y}_d - \sum_{j=1}^{N} a_{ij}K(t)(f_{j,1}(x_i) + x_{j,2})\Big)\Big) - \frac{1}{\ell_{i,1}}\tilde{P}_{i,1}^{\mathrm{T}}\dot{\hat{\mathrm{P}}}_{i,1}. \qquad (24)$$

由模糊逻辑系统的研究可得

$$g_{i,1}(x_i) = (b_i + d_i)K(t)f_{i,1}(x_i) - b_i\dot{y}_d - \sum_{j=1}^{N} a_{ij}K(t)(f_{j,1}(x_i) + x_{i,2}) \leqslant \theta_{i,1}^{\mathrm{T}}\phi_{i,1} + \chi_{i,1}, \qquad (25)$$

则有

$$\dot{V}_{i,1} \leqslant z_{i,1}\lambda_i K(t)\alpha_{i,1}(b_i + d_i) - \frac{1}{\ell_{i,1}}\tilde{P}_{i,1}^{\mathrm{T}}\dot{\hat{P}}_{i,1} + \varOmega_{i,1}, \qquad (26)$$

其中$\varOmega_{i,1} = z_{i,1}\dot{\lambda}_i e_i + z_{i,1}z_{i,2}\lambda_i K(t)(b_i + d_i) + z_{i,1}\lambda_i\theta_{i,1}^{\mathrm{T}}\phi_{i,1} + z_{i,1}\lambda_i\chi_{i,1}$.

应用引理4, 可得

$$\varOmega_{i,1} \leqslant \frac{z_{i,1}^2 e_i^2}{2} + \frac{z_{i,1}^2\lambda_i^2 K(t)^2(b_i + d_i)^2}{2} + \frac{z_{i,1}^2\lambda_i^2}{2} + \frac{z_{i,1}^2\lambda_i^2\|\theta_{i,1}\|^2\|\phi_{i,1}\|^2}{2a_{i,1}^2} + \frac{z_{i,2}^2}{2} + \frac{\dot{\lambda}_{i,\max}^2}{2} + \frac{a_{i,1}^2}{2} + \frac{\chi_{i,1}^2}{2} \leqslant z_{i,1}^2 P_{i,1}\varpi_{i,1} + \frac{z_{i,2}^2}{2} + \varDelta_{i,1}. \qquad (27)$$

其中: $\varDelta_{i,1} = \dot{\lambda}_{i,\max}^2/2 + a_{i,1}^2/2 + \varepsilon_{i,1}^2/2$, $P_{i,1} = \max\{K(t)^2(b_i + d_i)^2, \|\theta_{i,1}\|^2, 1\}$, $\varpi_{i,1} = e_i^2/2 + \lambda_i^2(1 + \|\phi_{i,1}\|^2/(2a_{i,1}^2))$, $a_{i,1} > 0$为设计参数.

虚拟控制器$\alpha_{i,1}$设计如下:

$$\alpha_{i,1} = N(k)\bar{\alpha}_{i,1}. \qquad (28)$$

其中: $\dot{k} = \gamma\bar{\alpha}_{i,1}z_{i,1}$, $N(k)$为设计的Nussbaum函数, $\gamma > 0$为设计参数, $\bar{\alpha}_1$设计在后续给出.

由式(26)～(28)可得

$$z_{i,1}\lambda_i K(t)\alpha_{i,1}(b_i + d_i) = \frac{\lambda_i(b_i + d_i)}{\gamma}(K(t)N(k) + 1)\dot{k} - \lambda_i(b_i + d_i)\bar{\alpha}_{i,1}z_{i,1}. \qquad (29)$$

$\bar{\alpha}_{i,1}$和参数自适应律$\dot{\hat{P}}_{i,1}$设计如下:

$$\bar{\alpha}_{i,1} = \frac{1}{b_i + d_i}(c_{i,1}e_i + \hat{P}_{i,1}\varpi_{i,1}e_i), \qquad (30)$$

$$\dot{\hat{P}}_{i,1} = \ell_{i,1}\varpi_{i,1}z_{i,1}^2 - s_{i,1}\hat{P}_{i,1}, \qquad (31)$$

其中$s_{i,1}$为设计参数.

式(26)可进一步转化为

$$\dot{V}_{i,1} \leqslant -c_{i,1}z_{i,1}^2 + \frac{z_{i,2}^2}{2} + \frac{s_{i,1}\tilde{P}_{i,1}^{\mathrm{T}}\hat{P}_{i,1}}{\ell_{i,1}} + \frac{\lambda_i(b_i + d_i)}{\gamma}(K(t)N(k) + 1)\dot{k} + \varDelta_{i,1}. \qquad (32)$$

step k ($k = 2, 3, \ldots, n-1$): 类似地, 构造如下Lyapunov函数:

$$V_{i,k} = V_{i,k-1} + \frac{1}{2}z_{i,k}^2 + \frac{1}{2\ell_{i,k}}\tilde{P}_{i,k}^2. \qquad (33)$$

由式(28)可得

$$\dot{\alpha}_{i,k-1} = \sum_{l=1}^{k-1}\frac{\partial\alpha_{i,k-1}}{\partial x_{i,l}}\dot{x}_{i,l} + \sum_{l=1}^{k-1}\frac{\partial\alpha_{i,k-1}}{\partial x_{j,l}}\dot{x}_{j,l} + \frac{\partial\alpha_{i,k-1}}{\partial y_{i,d}}\dot{y}_{i,d} + \sum_{l=1}^{k-1}\frac{\partial\alpha_{i,k-1}}{\partial\hat{P}_{i,l}}\dot{\hat{P}}_{i,l}. \qquad (34)$$

类似地, 由模糊逻辑系统的研究可得

$$g_{i,k}(x_i) = f_{i,k} - \sum_{l=1}^{k-1}\frac{\partial\alpha_{i,k-1}}{\partial x_{i,l}}\dot{x}_{i,l} - \sum_{l=1}^{k-1}\frac{\partial\alpha_{i,k-1}}{\partial x_{j,l}}\dot{x}_{j,l} - \frac{\partial\alpha_{i,k-1}}{\partial y_{i,d}}\dot{y}_{i,d} = \theta_{i,k}^{\mathrm{T}}\phi_{i,k} + \varepsilon_{i,k}. \qquad (35)$$

结合式(33)～(35),可得

$$V_{i,k} \leqslant -\sum_{l=1}^{k-1} c_{i,k-1} z_{i,k-1}^2 - \sum_{l=1}^{k-1} \frac{s_{i,l}\tilde{P}_{i,l}^{\mathrm{T}}\hat{P}_{i,l}}{\ell_{i,l}} + \frac{\lambda_i(b_i+d_i)}{\gamma}(K(t)N(k)+1)\dot{k} + z_{i,k}\Big(\frac{z_{i,k}}{2} + \alpha_{i,k} - \sum_{l=1}^{k-1}\frac{\partial\alpha_{i,k-1}}{\partial\hat{P}_{i,l}}\dot{\hat{P}}_{i,l}\Big) + \Omega_{i,k} - \frac{1}{\ell_{i,k}}\tilde{P}_{i,k}^{\mathrm{T}}\dot{\hat{P}}_{i,k} + \Delta_{i,k-1}. \tag{36}$$

其中: $\Omega_{i,k} = z_{i,k}z_{i,k+1} + \theta_{i,k}^{\mathrm{T}}\phi_{i,k}z_{i,k} + \varepsilon_{i,k}z_{i,k}, \varpi_{i,k} = 1 + \dfrac{\|\theta_{i,k}\|^2}{2a_{i,k}^2}, P_{i,k} = \max\{1, \|\theta_{i,k}\|^2\}$.

虚拟控制器$\alpha_{i,k}$和自适应律$\dot{\hat{P}}_{i,k}$设计如下:

$$\alpha_{i,k} = -\Big(c_{i,k} + \frac{1}{2}\Big)z_{i,k} + \sum_{l=1}^{k-1}\frac{\partial\alpha_{i,k-1}}{\partial\hat{P}_{i,l}}\dot{\hat{P}}_{i,l} - \hat{P}_{i,k}\varpi_{i,k}z_{i,k}, \tag{37}$$

$$\dot{\hat{P}}_{i,k} = \ell_{i,k}\varpi_{i,k}z_{i,k}^2 - s_{i,k}\hat{P}_{i,k}. \tag{38}$$

则式(36)可转换为如下形式:

$$V_{i,k} \leqslant -\sum_{l=1}^{k} c_{i,l}z_{i,l}^2 + \frac{z_{i,k+1}^2}{2} - \sum_{l=1}^{k}\frac{s_{i,l}\tilde{P}_{i,l}^{\mathrm{T}}\hat{P}_{i,l}}{\ell_{i,l}} + \frac{\lambda_i(b_i+d_i)}{\gamma}(K(t)N(k)+1)\dot{k} + \Delta_{i,k}. \tag{39}$$

其中$\Delta_{i,k} = \Delta_{i,k-1} + a_{i,k}^2/2 + \varepsilon_{i,k}^2/2$.

step n: 定义

$$\bar{e}(t) = w_i(t) - u_i(t),\ \beta_i = -\sum_{l=1}^{n-1}\frac{\partial\alpha_{i,n-1}}{\partial\hat{P}_{i,l}}\dot{\hat{P}}_{i,l},$$

$$\varpi_{i,n} = 1 + \frac{\|\theta_{i,n}\|^2}{2a_{i,n}^2},\ K_{i,n} = \max\{1, \|\phi_{i,n}\|^2\}.$$

所采用的事件触发控制机制如下:

$$w_i(t) = -(1+m)\Big(c_{i,n}z_{i,n} + \frac{1}{2}z_{i,n} + \hat{P}_{i,k}\varpi_{i,k}z_{i,k} + \beta\tanh\Big(\frac{z_{i,n}\beta}{\tau}\Big)\Big) - \frac{(1+m)z_{i,n}}{2(1-m)^2};$$

$$\dot{\hat{P}}_{i,n} = \ell_{i,n}\varpi_n z_{i,n}^2 - s_{i,n}\hat{P}_{i,n};$$

$$u_i(t) = w_i(t_k),\ \forall t \in [t_k, t_{k+1});$$

$$t_{k+1} = \inf\{t \in R||\bar{e}(t)| \geqslant m|u(t)| + m_1\}. \tag{40}$$

其中$0 < m < 1$和m_1均为正设计参数.

设$|\kappa_1(t)| < 1, |\kappa_2(t)| < 1$为时变函数,结合式(40),可得

$$u_i(t) = \frac{w_i(t)}{1+\kappa_1(t)m} - \frac{\kappa_2(t)m_1}{1+\kappa_1(t)m}. \tag{41}$$

选取Lyapunov函数V_n为

$$V_{i,n} = V_{i,n-1} + \frac{1}{2}z_{i,n}^2 + \frac{1}{2\ell_{i,n}}\tilde{P}_{i,n}^{\mathrm{T}}\tilde{P}_{i,n}. \tag{42}$$

由式(37)可得

$$\dot{\alpha}_{i,n-1} = \sum_{l=1}^{n-1}\frac{\partial\alpha_{i,n-1}}{\partial x_{i,l}}\dot{x}_{i,l} + \sum_{l=1}^{n-1}\frac{\partial\alpha_{i,n-1}}{\partial x_{j,l}}\dot{x}_{j,l} + \frac{\partial\alpha_{i,n-1}}{\partial y_{i,d}}\dot{y}_{i,d} + \sum_{l=1}^{n-1}\frac{\partial\alpha_{i,n-1}}{\partial\hat{P}_{i,l}}\dot{P}_{i,l}. \tag{43}$$

由模糊逻辑系统的研究可知

$$g_{i,n}(x_i) = f_{i,n} - \sum_{l=1}^{n-1}\frac{\partial\alpha_{i,n-1}}{\partial x_{i,l}}\dot{x}_{i,l} - \sum_{l=1}^{n-1}\frac{\partial\alpha_{i,n-1}}{\partial x_{j,l}}\dot{x}_{j,l} - \frac{\partial\alpha_{i,n-1}}{\partial y_{i,d}}\dot{y}_{i,d} = \theta_{i,n}^{\mathrm{T}}\phi_{i,n} + \varepsilon_{i,n}. \tag{44}$$

结合式(40)～(44),可得

$$\dot{V}_{i,n} \leqslant -\sum_{l=1}^{n} c_l z_{i,l}^2 - \sum_{l=1}^{n}\frac{s_{i,l}\tilde{P}_{i,l}^{\mathrm{T}}\tilde{P}_{i,l}}{2\ell_{i,l}} + \sum_{l=1}^{n}\frac{s_{i,l}P_{i,l}^{T}P_{i,l}}{2\ell_{i,l}} + \frac{\lambda_i(b_i+d_i)}{\gamma}(K(t)N(k)+1)\dot{k} + \Delta_{i,n} + \frac{m_1^2(t)}{2} + 0.2785\tau \leqslant -\rho V_{i,n} + \Delta_i + \frac{\lambda_i(b_i+d_i)}{\gamma}(K(t)N(k)+1)\dot{k}. \tag{45}$$

其中

$$\Delta_{i,n} = \Delta_{i,n-1} + \frac{a_{i,n}^2}{2} + \frac{\varepsilon_{i,n}^2}{2},$$

$$\Delta_i = \Delta_{i,n} + \sum_{l=1}^{n}\frac{s_{i,l}P_{i,l}^{\mathrm{T}}P_{i,l}}{2\ell_{i,l}} + \frac{m_1^2(t)}{2} + 0.2785\lambda,$$

$$\rho = \min\{2c_{i,1}, \ldots, 2c_{i,n}, 2s_{i,1}, \ldots, 2s_{i,n}\} > 0.$$

注1 由文献[30]可知,对于任意$\beta \in R, \lambda > 0$, $0 \leqslant \beta - \beta\tanh(\beta/\lambda) \leqslant 0.2785\lambda$ 恒成立, $-\beta\tanh(\beta/\lambda) \leqslant 0$.

定理1 在虚拟领导者的输出信号y_d及其n阶导数都是连续且有界以及至少存在一个跟随者与领导者之间存在信息交互成立的条件下,在非线性转换函数(15)、虚拟控制器(28)、(30)、(37)、参数自适应律(31)、(38)、事件触发机制(40)等作用下,带输出死区的多智能体系统(1)可满足以下条件:

1) 系统所有信号均为半全局一致最终有界;

2) 事件触发的时间间隔$\{t_{k+1} - t_k\}$存在下界$t^* > 0$,可以有效避免Zeno现象;

3) 系统同步误差e_i可以在预设时间T内收敛于紧集Ω_i.

证明 构造Lyapunov函数

$$V = \sum_{i=1}^{N}\sum_{k=1}^{n}\Big(\frac{1}{2}z_{i,k}^2 + \frac{1}{2\ell_{i,k}}\tilde{P}_{i,k}^{\mathrm{T}}\tilde{P}_{i,k}\Big). \tag{46}$$

由式(45),对V求导可得

$$\dot{V} \leqslant -\rho V + \Delta + \frac{\lambda(b+d)}{\gamma}(K(t)N(k)+1)\dot{k}. \tag{47}$$

其中: $\lambda(b+d)=\sum_{i=1}^{N}\lambda_i(b_i+d_i), \Delta=\sum_{i=1}^{N}\Delta_i$.

对式(47)在区间$[0,t]$积分,可得

$$V\leqslant V(0)\mathrm{e}^{-\rho t}+\frac{\Delta}{\rho}(1-\mathrm{e}^{-\rho t})+\frac{\lambda(b+d)\mathrm{e}^{-\rho t}}{\gamma}\int_0^t(K(t)N(k)+1)\dot{k}\mathrm{e}^{\rho\tau}\mathrm{d}\tau. \quad (48)$$

由引理3可知, $V(t)$、$k(t)$以及$\int_0^t(K(t)N(k)+1)\dot{k}\mathrm{e}^{\rho\tau}\mathrm{d}\tau$在$[0,t_f]$上有界. 由于

$$\int_0^t(K(t)N(k)+1)\dot{k}\mathrm{e}^{-\rho(t-\tau)}\mathrm{d}\tau\leqslant\int_0^t(K(t)N(k)+1)\dot{k}\mathrm{d}\tau, \quad (49)$$

可得$\int_0^t(K(t)N(k)+1)\dot{k}\mathrm{e}^{-\rho(t-\tau)}\mathrm{d}\tau$在$[0,t_f]$也是有界的. 定义

$$\varsigma=\max_{t\in[0,t_f)}\left|\int_0^t(K(t)N(k)+1)\dot{k}\mathrm{e}^{-\rho(t-\tau)}\mathrm{d}\tau\right|, \quad (50)$$

结合式(48) ~ (50),可得

$$\frac{z_1^2}{2}\leqslant V(t)\leqslant V(0)\mathrm{e}^{-\rho t}+\frac{\Delta}{\rho}(1-\mathrm{e}^{-\rho t})+\frac{\lambda(b+d)\varsigma}{\gamma}. \quad (51)$$

由式(51)可知,系统所有信号都是半全局一致最终有界的. 因为$\bar{e}_i(t)=w_i(t)-u_i(t), t\in[t_k,t_{k+1})$, $u_i(t)$在触发间隔内保持上一触发时刻的控制信号值, $u_i(t)$为常数,则有

$$\frac{\mathrm{d}}{\mathrm{d}t}|\bar{e}_i|=\frac{\mathrm{d}}{\mathrm{d}t}(\bar{e}_i\times\bar{e}_i)^{\frac{1}{2}}=\mathrm{sign}(\bar{e}_i)\dot{\bar{e}}_i\leqslant|\dot{w}_i(t)|. \quad (52)$$

$w_i(t)$由系统有界信号构成,因此$|\dot{w}_i(t)|\leqslant\varGamma$存在,且$\varGamma>0$,有

$$\lim_{t\to t_{k+1}}\bar{e}_i(t)=m|u(t)|+m_1\geqslant m_1, \bar{e}_i(t_k)=0,$$

$$\frac{\mathrm{d}}{\mathrm{d}t}|\bar{e}_i|=\lim_{t_k\to t_{k+1}}\frac{\bar{e}_i(t_{k+1})-\bar{e}_i(t_k)}{t_{k+1}-t_k}=\frac{m|u(t)|+m_1}{t^*}.$$

综上可得$(m|u(t)|+m_1)/t^*\leqslant\varGamma$, 即$t^*\geqslant(m|u(t)|+m_1)/\varGamma\geqslant m_1/\varGamma>0$. t^*为事件触发间隔的下界. 显然, Zeno现象可以被有效避免.

令

$$\bar{\Delta}=\Delta+\frac{\lambda(b+d)}{\gamma}(K(t)N(k)+1)\dot{k},$$

则式(46)可改写为

$$\dot{V}\leqslant-\rho V+\bar{\Delta}. \quad (53)$$

由文献[31],通过选取适当的设计参数,可得$|z_{i,1}|\leqslant\sqrt{2\bar{\Delta}/\rho}$. 由式(21), $|e_i|=\lambda_i^{-1}|z_{i,1}|\leqslant\lambda_i^{-1}\sqrt{\dfrac{2\bar{\Delta}}{\rho}}$,有

$$|e_i|\leqslant\begin{cases}\left(1-\dfrac{\varTheta}{\varPsi}\right)\left(\dfrac{T-t}{T}\right)^2\mathrm{e}^{-\nu t}\sqrt{\dfrac{2\bar{\Delta}}{\rho}}+\dfrac{\varTheta}{\varPsi}\sqrt{\dfrac{2\bar{\Delta}}{\rho}},\\ \quad 0\leqslant t<T;\\ \dfrac{\varTheta}{\varPsi}\sqrt{\dfrac{2\bar{\Delta}}{\rho}},\ t\geqslant T.\end{cases} \quad (54)$$

式(54)表明,多智能体系统的同步误差将在预设时间T内收敛于紧集$\varOmega_i=\left\{e_i\middle||e_i|\leqslant\dfrac{\varTheta}{\varPsi}\sqrt{\dfrac{2\bar{\Delta}}{\rho}}\right\}$,其收敛速率将不低于$\left(\dfrac{T-t}{T}\right)^2\mathrm{e}^{-\nu t}$. □

注2 参数$\bar{\Delta}$中包含着非线性转换函数的值和设计参数γ等,可通过调整相关参数的值进一步调整$\bar{\Delta}$,但与此同时仍需要综合考虑系统控制力、同步误差、事件触发效果等各方面因素以平衡性能.

3 实验仿真

考虑由1个领导者和4个跟随者组成的多智能体系统,其通信拓朴图如图1所示.

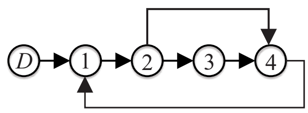

图1 通信拓扑图

3.1 数值仿真

考虑带有图1通信拓扑结构的多智能体系统,其跟随者动态建模如下:

$$\begin{cases}\dot{x}_{i,1}=x_{i,2}+f_{i,1}(x_{i,1}),\\ \dot{x}_{i,2}=u_i+f_{i,2}(x_{i,2}),\\ y_i=\mathrm{DZ}(x_{i,1}).\end{cases}$$

其中

$$f_{i,1}(x_i)=0.2\sin(x_{i,1}),\ f_{i,2}(x_i)=0.2\sin(x_{i,1}^2x_{i,2}),$$

给定参考轨迹信号为$y_d=\sin t+\sin(0.5t)$.

系统输出死区特性$y_i=\mathrm{DZ}(x_{i,1})$定义为

$$\mathrm{DZ}(x_{i,1})=\begin{cases}0.7(x_{i,1}-0.02),\ x_{i,1}>0.02;\\ 0,\ -0.023<x_{i,1}<0.02;\\ x_{i,1}+0.023,\ x_{i,1}<-0.023.\end{cases}$$

数值仿真的初始值设置如下: $\hat{K}_1(0)=0, \hat{K}_2(0)=0, x_{i,1}(0)=[0.1,0.2,0.3,0.4], x_{i,2}(0)=[0,0,0,0], u(0)=[0,0,0,0]$.

仿真参数设置如下: $b_1=1, a_{21}=1.5, a_{32}=1, a_{43}=1, a_{42}=0.01, a_{14}=0.01, c_1=[40,70,45,45], c_2=[11,25,15,15], T=1.5, v=0.5, \varTheta=0.3, \varPsi=0.05, m=0.2, \tau=0.9, m_1=0.1, a_1=10, a_2=10, \ell_1=1, \ell_2=2, s_{i,1}=10, s_{i,2}=10$.

仿真结果如图2～图5所示. 图2为给定参考轨迹与各个智能体的输出轨迹,跟随者在较短时间内实现了轨迹跟踪,状态有界且误差较小. 图3为多智能体系统的同步误差,其在1.04 s后进入5 %的误差带范围,并一直保持在该误差范围内. 图4为系统的控制输入,由图4可见,在遭受输出死区现象时,控制力增大对其进行补偿控制,然后迅速调整,达到一个趋于零的水平. 图5为各个智能体事件触发次数的具体情况,其触发率分别为传统方法的22.0 %、34.8 %、29.6 %、31.2 %. 显然,该系统不存在Zeno现象,且相较于传统方法,该方法可有效降低系统控制信号的传输频率,减轻控制传输资源压力.

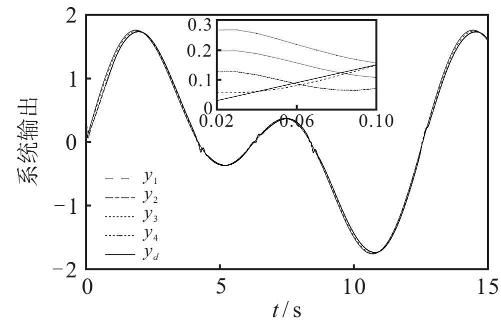

图 2　系统输出轨迹(数值仿真)

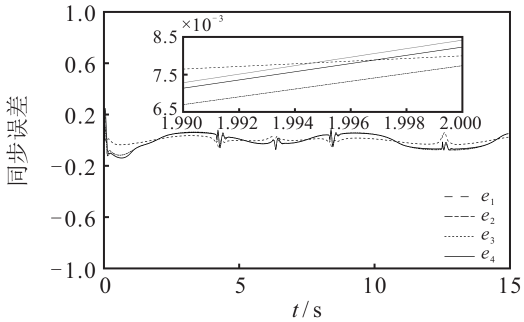

图 3　同步误差(数值仿真)

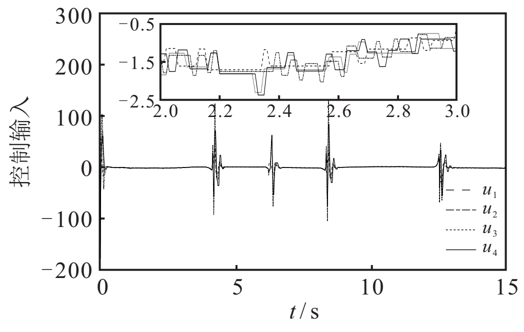

图 4　系统控制输入(数值仿真)

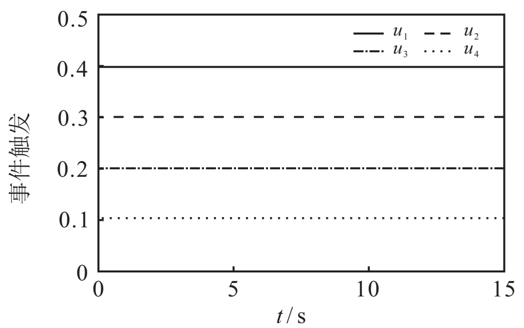

图 5　事件触发情况(数值仿真)

3.2　实例仿真

为验证所提出方法在实际系统中的效果,本节将其作用于如下带有输出死区特性的机械臂系统(由4个单关节机械臂构成,系统通信拓扑结构见图1):

$$J\ddot{q}_i + B\dot{q}_i + Mgl\sin(q_i) = u(t),$$

$$Q_i(t) = \mathrm{DZ}(q_i).$$

其中: 转动惯量 $J = 1$, 阻尼系数 $B = 1$, 连杆总质量 $M = 0.1\,\mathrm{kg}$, 重力加速度 $g = 10\,\mathrm{m/s^2}$, 连杆长度 $l = 1\,\mathrm{m}$; Q_i 为多机械臂系统的输出, 即系统的输出死区 $\mathrm{DZ}(q_i)$, 其输入为 q_i.

实例仿真初始值设置、仿真参数与数值仿真一致. 仿真结果如图6～图9所示. 实例仿真结果与数值仿真结果基本一致. 由图6可见,多智能体系统的各个子系统输出轨迹可以很好地跟踪参考信号,系统状态有界. 图7表明,系统同步误差较小,在1.08 s后同步误差低于5 %,可以实现在预设时间内到达稳态的控制目标. 图8和图9分别为系统的控制输入以及事件触发频次. 由图9可知,Zeno现象被有效避免了. 各个智能体事件触发的频次分别为295、500、408、412,约为传统控制信号传输方法的19.7 %、33.3 %、27.2 %、27.5 %. 显然,带输出死区的多智能体系统可预设时间事件触发式协同控制方法能够在保证系统性能的基础上,节约系统控制传输资源,同时保证系统在预设时间内到达稳定状态.

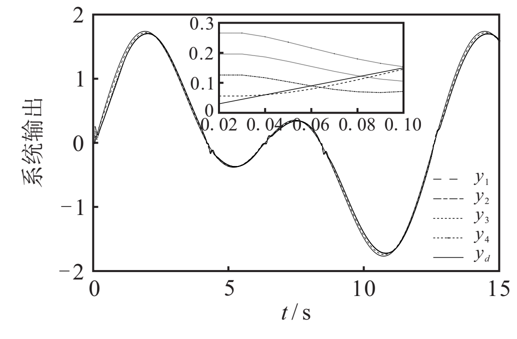

图 6　系统输出轨迹(实例仿真)

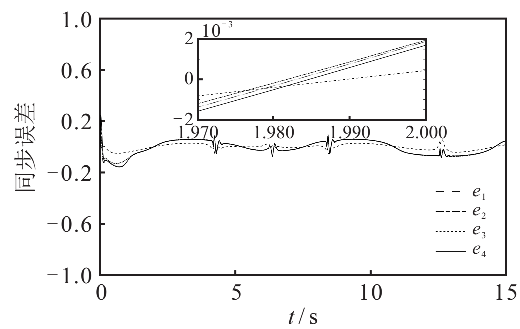

图 7　同步误差(实例仿真)

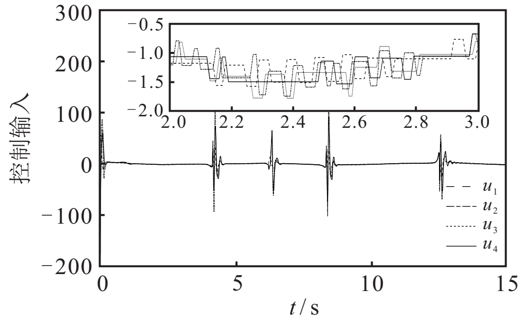

图 8 系统控制输入(实例仿真)

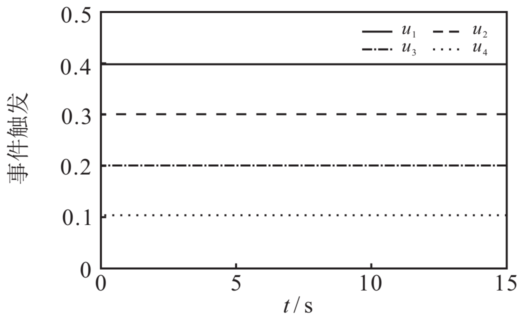

图 9 事件触发情况(实例仿真)

4 结 论

本文考虑了带有输出死区的多智能体系统一致性控制问题. 首先,利用Nussbaum函数对系统的输出死区特性进行补偿;然后,通过事件触发机制解决因输出死区补偿给系统带来的控制传输资源紧张问题,节省系统资源;最后,在控制设计中引入一类转换函数,对系统的误差变量进行适当的放缩,以进一步提高系统性能. 仿真实验结果表明,所提出方法可以使得系统同步误差在预设时间内收敛于紧集,保证了跟踪性能,同时可以有效节省通讯带宽资源.

参考文献(References)

[1] Ma L, Huo X, Zhao X D, et al. Adaptive neural control for switched nonlinear systems with unknown backlash-like hysteresis and output dead-zone[J]. Neurocomputing, 2019, 357: 203-214.

[2] Shi X C, Lim C C, Shi P, et al. Adaptive neural dynamic surface control for nonstrict-feedback systems with output dead zone[J]. IEEE Transactions on Neural Networks and Learning Systems, 2018, 29(11): 5200-5213.

[3] Liu Z, Lai G Y, Zhang Y, et al. Adaptive fuzzy tracking control of nonlinear time-delay systems with dead-zone output mechanism based on a novel smooth model[J]. IEEE Transactions on Fuzzy Systems, 2015, 23(6): 1998-2011.

[4] Wang F, Liu Z, Lai G Y. Fuzzy adaptive control of nonlinear uncertain plants with unknown dead zone output[J]. Fuzzy Sets and Systems, 2015, 263: 27-48.

[5] Wang J H, Liu Z, Chen C L P, et al. Event-triggered neural adaptive failure compensation control for stochastic systems with dead-zone output[J]. Nonlinear Dynamics, 2019, 96(3): 2179-2196.

[6] Dimarogonas D V, Frazzoli E, Johansson K H. Distributed event-triggered control for multi-agent systems[J]. IEEE Transactions on Automatic Control, 2012, 57(5): 1291-1297.

[7] Guo G, Ding L, Han Q L. A distributed event-triggered transmission strategy for sampled-data consensus of multi-agent systems[J]. Automatica, 2014, 50(5): 1489-1496.

[8] 孙长银, 穆朝絮. 多智能体深度强化学习的若干关键科学问题[J]. 自动化学报, 2020, 46(7): 1301-1312.
(Sun C Y, Mu C X. Important scientific problems of multi-agent deep reinforcement learning[J]. Acta Automatica Sinica, 2020, 46(7): 1301-1312.)

[9] Hu W F, Liu L, Feng G. Consensus of linear multi-agent systems by distributed event-triggered strategy[J]. IEEE Transactions on Cybernetics, 2016, 46(1): 148-157.

[10] Li X M, Zhou Q, Li P S, et al. Event-triggered consensus control for multi-agent systems against false data-injection attacks[J]. IEEE Transactions on Cybernetics, 2020, 50(5): 1856-1866.

[11] 董滔, 李小丽, 赵大端. 基于事件触发的三阶离散多智能体系统一致性分析[J]. 自动化学报, 2019, 45(7): 1366-1372.
(Dong T, Li X L, Zhao D D. Event-triggered consensus of third-order discrete-time multi-agent systems[J]. Acta Automatica Sinica, 2019, 45(7): 1366-1372.)

[12] Yang R H, Zhang H, Feng G, et al. Robust cooperative output regulation of multi-agent systems via adaptive event-triggered control[J]. Automatica, 2019, 102: 129-136.

[13] 杨若涵, 张皓, 严怀成. 基于事件触发的拓扑切换异构多智能体协同输出调节[J]. 自动化学报, 2017, 43(3): 472-477.
(Yang R H, Zhang H, Yan H C. Event-triggered cooperative output regulation of heterogeneous multi-agent systems with switching topology[J]. Acta Automatica Sinica, 2017, 43(3): 472-477.)

[14] Mu R, Wei A R, Li H T, et al. Event-triggered leader-following consensus for multi-agent systems with external disturbances under fixed and switching topologies[J]. IET Control Theory & Applications, 2020, 14(11): 1486-1496.

[15] 刘洋, 井元伟, 刘晓平, 等. 非线性系统有限时间控制研究综述[J]. 控制理论与应用, 2020, 37(1): 1-12.
(Liu Y, Jing Y W, Liu X P, et al. Survey on finite-time control for nonlinear systems[J]. Control Theory & Applications, 2020, 37(1): 1-12.)

[16] 丁世宏, 李世华. 有限时间控制问题综述[J]. 控制与决策, 2011, 26(2): 161-169.
(Ding S H, Li S H. A survey for finite-time control problems[J]. Control and Decision, 2011, 26(2): 161-169.)
[17] Bhat S P, Bernstein D S. Lyapunov analysis of finite-time differential aligns[C]. Proceedings of 1995 American Control Conference. Seattle, 1995: 1831-1832.
[18] Bhat S P, Bernstein D S. Finite-time stability of homogeneous systems[C]. Proceedings of the 1997 American Control Conference. Albuquerque, 1997: 2513-2514.
[19] Sui S, Chen C L P, Tong S C. Fuzzy adaptive finite-time control design for nontriangular stochastic nonlinear systems[J]. IEEE Transactions on Fuzzy Systems, 2019, 27(1): 172-184.
[20] Wang F, Chen B, Sun Y M, et al. Finite-time fuzzy control of stochastic nonlinear systems[J]. IEEE Transactions on Cybernetics, 2020, 50(6): 2617-2626.
[21] 刘凡, 杨洪勇, 杨怡泽, 等. 带有不匹配干扰的多智能体系统有限时间积分滑模控制[J]. 自动化学报, 2019, 45(4): 749-758.
(Liu F, Yang H Y, Yang Y Z, et al. Finite-time integral sliding-mode control for multi-agent systems with mismatched disturbances[J]. Acta Automatica Sinica, 2019, 45(4): 749-758.)
[22] Li S H, Du H B, Lin X Z. Finite-time consensus algorithm for multi-agent systems with double-integrator dynamics[J]. Automatica, 2011, 47(8): 1706-1712.
[23] Lü H, He W L, Han Q L, et al. Finite-time containment control for nonlinear multi-agent systems with external disturbances[J]. Information Sciences, 2020, 512: 338-351.
[24] Mo L P, Yu Y G. Finite-time rotating encirclement control of multi-agent systems[J]. 自动化学报, 2017, 43(9): 1665-1672.
(Mo L P, Yu Y G. Finite-time rotating encirclement control of multi-agent systems[J]. Acta Automatica Sinica, 2017, 43(9): 1665-1672.)
[25] Ren C C, Nie R, He S P. Finite-time positiveness and distributed control of Lipschitz nonlinear multi-agent systems[J]. Journal of the Franklin Institute, 2019, 356(15): 8080-8092.
[26] Zhang H W, Lewis F L. Adaptive cooperative tracking control of higher-order nonlinear systems with unknown dynamics[J]. Automatica, 2012, 48(7): 1432-1439.
[27] Zhang C L, Chen Z C, Wang J H, et al. Fuzzy adaptive two-bit-triggered control for a class of uncertain nonlinear systems with actuator failures and dead-zone constraint[J]. IEEE Transactions on Cybernetics, 2021, 51(1): 210-221.
[28] Ge S S, Hong F, Lee T H. Adaptive neural control of nonlinear time-delay systems with unknown virtual control coefficients[J]. IEEE Transactions on Systems, Man, and Cybernetics — Part B, 2004, 34(1): 499-516.
[29] Young W H. On classes of summable functions and their Fourier series[J]. Proceedings of the Royal Society of London Series A, Containing Papers of a Mathematical and Physical Character, 1912, 87(594): 225-229.
[30] Ren B B, San P P, Ge S S, et al. Adaptive dynamic surface control for a class of strict-feedback nonlinear systems with unknown backlash-like hysteresis[J]. 2009 American Control Conference, 2009: 4482-4487.
[31] Xing L T, Wen C Y, Liu Z T, et al. Event-triggered adaptive control for a class of uncertain nonlinear systems[J]. IEEE Transactions on Automatic Control, 2017, 62(4): 2071-2076.

作者简介

王建晖 (1984−), 男, 讲师, 博士, 从事智能控制、振动控制等研究, E-mail: jhwang@gzhu.edu.cn;

邹涛 (1975−), 男, 教授, 博士生导师, 从事工业实时优化、先进过程控制等研究, E-mail: tzou@gzhu.edu.cn;

张春良 (1964−), 男, 教授, 博士生导师, 从事设备状态监测与故障诊断、智能控制等研究, E-mail: nhzcl@163.com;

穆朝絮 (1984−), 女, 教授, 博士生导师, 从事非线性控制理论及应用、智能自适应控制等研究, E-mail: cxmu@tju.edu.cn;

刘治 (1977−), 男, 教授, 博士生导师, 从事自适应控制、智能机器人等研究, E-mail: lz@gdut.edu.cn.

(责任编辑: 郑晓蕾)